Molybdenum Trioxide Nanoparticles with Intrinsic Sulfite Oxidase Activity

Ruben Ragg,[†] Filipe Natalio,[‡] Muhammad Nawaz Tahir,[†] Henning Janssen,[§] Anubha Kashyap,[§] Dennis Strand,[§] Susanne Strand,[§] and Wolfgang Tremel[†,*]

[†]Institut für Anorganische Chemie und Analytische Chemie, Johannes-Gutenberg-Universität, Duesbergweg 10—14, D-55099 Mainz, Germany, [‡]Institut für Chemie — Anorganische Chemie, Martin-Luther Universität Halle-Wittenberg, Kurt Mothes Straße 2, D-06120 Halle, Germany, and [§]Medizinische Klinik and Poliklinik, Universitätsmedizin, Johannes Gutenberg-Universität, Obere Zahlbacher Strasse 63, D-55131 Mainz, Germany. The manuscript was written through contributions of all authors. All authors have given approval to the final version of the manuscript.

ABSTRACT Sulfite oxidase is a mitochondria-located molybdenum-containing enzyme catalyzing the oxidation of sulfite to sulfate in the amino acid and lipid metabolism. Therefore, it plays a major role in detoxification processes, where defects in the enzyme cause a severe infant disease leading to early death with no efficient or cost-effective therapy in sight. Here we report that molybdenum trioxide (MoO_3) nanoparticles display an intrinsic biomimetic sulfite oxidase activity under physiological conditions, and, functionalized with a customized bifunctional ligand containing dopamine as anchor group and triphenylphosphonium ion as targeting agent, they selectively target the mitochondria while being highly dispersible in aqueous solutions. Chemically induced sulfite oxidase knockdown cells treated with MoO_3 nanoparticles recovered their sulfite oxidase activity *in vitro*, which makes MoO_3 nanoparticles a potential therapeutic for sulfite oxidase deficiency and opens new avenues for cost-effective therapies for gene-induced deficiencies.

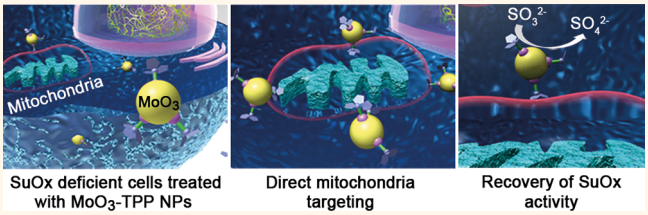

KEYWORDS: enzyme mimic · molybdenum oxide · sulfite oxidase · sulfite oxidase deficiency · nanoparticles · catalysis · biomimetics

Molybdenum trioxide (MoO_3) is a well-known model compound for selective oxidation catalysis.[1,2] Its catalytic properties depend on the crystal phase, surface structure, and especially particle size. Generally, nanoparticular MoO_3 is deposited and stabilized on different metal oxides, such as ZrO_2,[3] Al_2O_3,[4] or SiO_2.[5] Although the catalytic activity of MoO_3 is well documented, its biocatalytic behavior is virtually unknown, even though the presence of molybdenum in biological systems as key component of enzymes catalyzing redox and oxygen transfer reactions is well established.[6,7] In most of those enzymes Mo is utilized as part of the molybdenum cofactor (Moco), a Mo complex containing the molybdopterin ligand. In mammals, Moco is incorporated in several important enzymes, such as xanthine oxidase, aldehyde oxidase, nitrate reductase, mARC (mitochondrial amidoxime reducing component) and sulfite oxidase (SuOx),[7,8] which is a 104 kDa dimeric enzyme containing a C-terminal molybdopterin-binding domain with the metal center in its highest (Mo^{VI}) oxidation state. Located in the mitochondrial intermembrane space of liver and kidney cells it catalyzes the oxidation of sulfite to sulfate using ferricytochrome c as the physiological electron acceptor.[9] This reaction is biologically essential as the final step in the catabolism of sulfur-containing amino acids cysteine and methionine. Severe neurological damage and early childhood death result from a deficiency of SuOx activity (SOD) due to an inborn metabolic defect.[10] SuOx also functions in detoxifying exogenously supplied sulfite and sulfur dioxide (*e.g.*, pollution, preservatives).

The fundamental chemistry catalyzed by SuOx has been studied using several model compounds containing $[Mo^{VI}O_2]$ units involving phosphines as model substrates.[11,12] $[Bu_4N]_2[MoO_2(mnt)_2]$ (mnt = maleonitriledithiolene) catalyzes the oxidation of sulfite to sulfate,[13] but none of the biomimetic compounds have shown any cellular activity. There is growing evidence that nanoparticles can act as enzyme mimics.[14,15] On the basis of the established activity of MoO_3 as oxidation catalyst,[1−5,16] the reported antibacterial activity of MoO_3,[17] and the catalytic properties of SuOx model compounds,[10−12] we

* Address correspondence to tremel@uni-mainz.

Received for review March 3, 2014 and accepted April 4, 2014.

Published online April 04, 2014
10.1021/nn501235j

reasoned that MoO_3 nanoparticles might allow exploring MoO_3-catalyzed reactions such as the intracellular oxidation of sulfite to sulfate.

Here we demonstrate that surface functionalized MoO_3 nanoparticles exhibit an intrinsic biomimetic SuOx activity that allows intracellular oxidation of sulfite to sulfate. Given their small size and surface-targeting moiety triphenylphosphonium ion (TPP), functionalized MoO_3-TPP nanoparticles can cross the cellular membrane and accumulate specifically at the mitochondria (Figure 1b,c), allowing recovery (Figure 1d) of the SuOx activity of chemically induced SuOx knockdown liver cells (HepG2, a human hepatoblastoma cell line, Figure 1a).

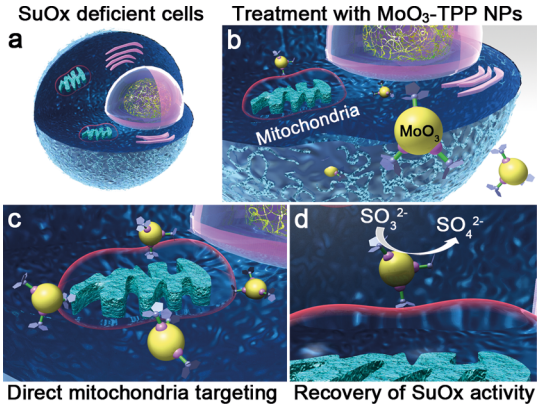

Figure 1. Mode of action of MoO_3 nanoparticles. (a) Hepatocytes are treated with sodium tungstate to induce SuOx deficiency *in vitro*. (b) SuOx deficient cells are treated with 2 nm TPP-surface functionalized MoO_3 nanoparticles. (c) Mitochondria are directly targeted, and nanoparticles accumulate in close proximity to the membrane. (d) Sulfite is oxidized to cellular innocuous sulfate by MoO_3 nanoparticles, and therefore SuOx activity is reconstituted and cells regain their detoxifying capacity.

RESULTS AND DISCUSSION

Synthesis and Characterization. MoO_3 nanoparticles[18] displayed a yellow color and an excellent dispersibility in water (Supporting Information Figure S1, inset). Powder X-ray diffraction (P-XRD) showed the presence of the hydrated form of monoclinic hydrogen molybdenum oxide ($H_2MoO_5 \cdot H_2O$, peroxymolybdate)[19] (Supporting Information Figure S1). Calcination (450 °C, 30 min) yielded orthorhombic α-MoO_3 (*Pbnm*) as a white powder (P-XRD, Supporting Information Figure S2) with equally high water dispersibility (Supporting Information Figure S2, inset). Transmission electron microscopy (TEM) images of the annealed powder showed the presence of MoO_3 nanoparticles (∅ ≈ 2 nm, Figure 2a). Scanning transmission electron microscopy (STEM) and energy-dispersive X-ray spectroscopy (EDX) confirmed the elemental composition (Figure 2b). Assays in simulated biological environment revealed that MoO_3 nanoparticles retain their structure after incubation in bovine serum (shown by P-XRD, Supporting Information Figure S3).

The calcinated nanoparticles were surface functionalized with a bifunctional ligand containing dopamine (Dopa) as anchor group and a TPP moiety that

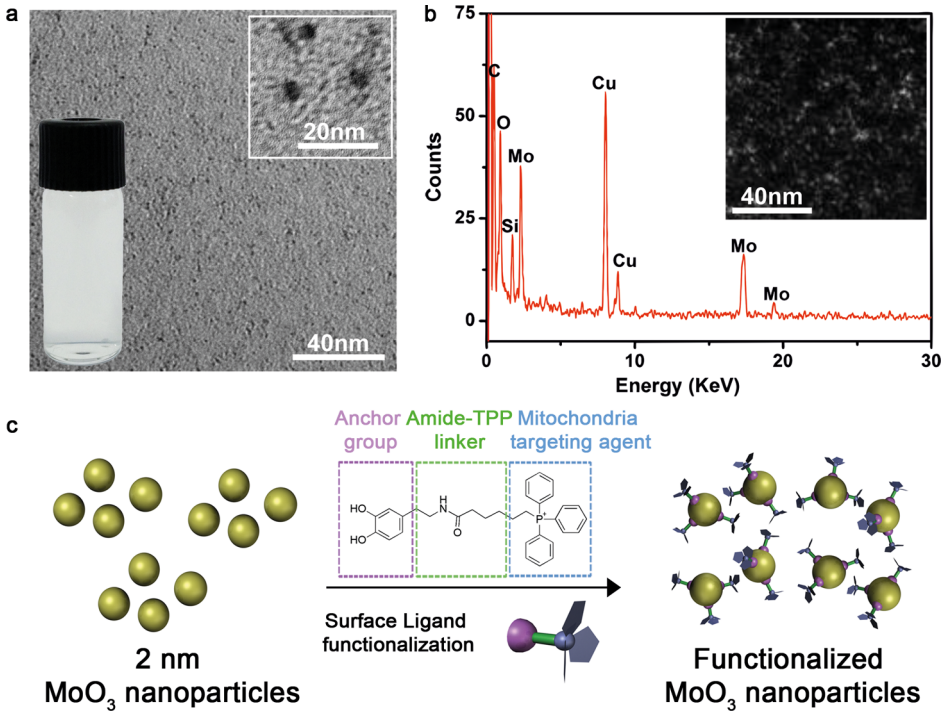

Figure 2. Mitochondria-specific surface functionalization of MoO_3 nanoparticles (∅ ≈ 2 nm). (a) TEM images of MoO_3 nanoparticles and digital photograph of a 0.5 mg/mL MoO_3-TPP nanoparticle dispersion in distilled water. (b) STEM image and elemental analysis by EDX of MoO_3 nanoparticles. (c) Surface functionalization of 2 nm MoO_3 nanoparticles with ligand containing dopamine as anchor group and TPP as mitochondria targeting agent.

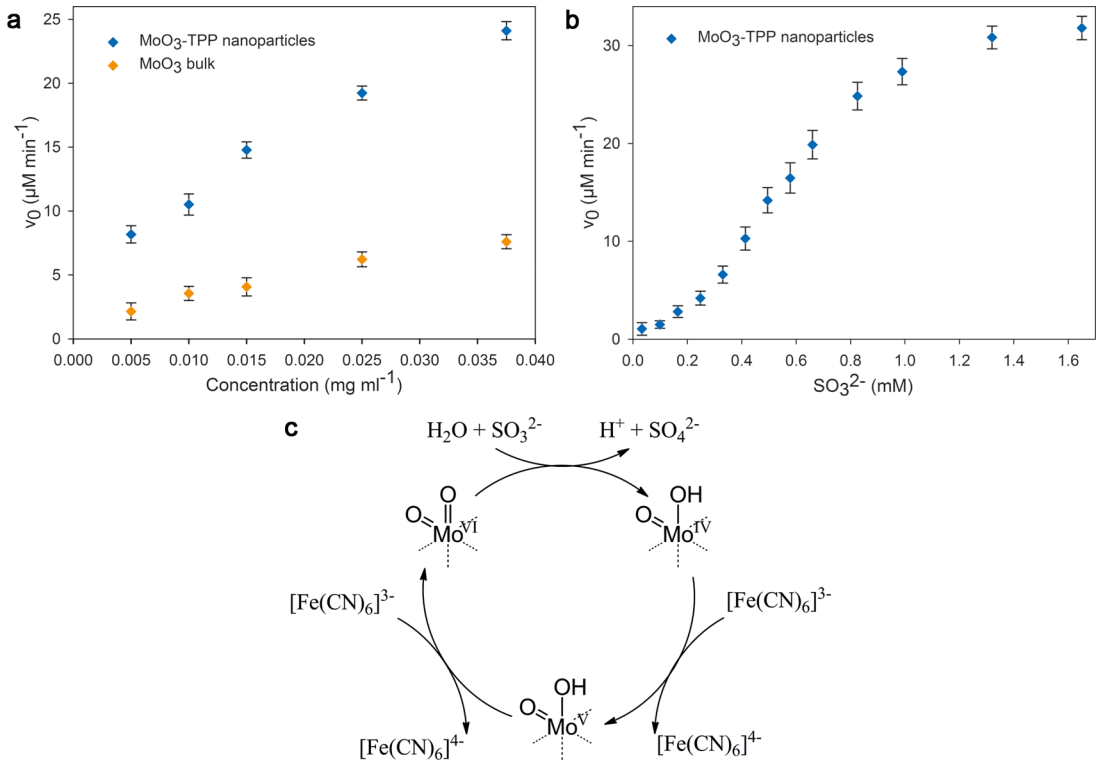

Figure 3. Concentration dependence and steady-state kinetics of MoO_3-TPP nanoparticles. (a) Concentration dependence of the sulfite oxidase activity of functionalized MoO_3-TPP nanoparticles (blue diamonds) and bulk MoO_3 (orange diamonds) in the presence of constant concentrations of SO_3^{2-} (0.66 mM) and potassium ferricyanide (0.33 mM). A 4-fold activity difference between nanoscale and bulk MoO_3 indicates the importance of a higher surface area for attaining higher catalytic efficiencies. (b) Variation of the SO_3^{2-} concentration (0.03−1.65 mM) while keeping the MoO_3-TPP nanoparticle (0.025 mg/mL) and ferricyanide (0.33 μM) concentrations constant. (c) Proposed catalytic sulfite oxidase mechanism for MoO_3 nanoparticles.

permits cell-membrane crossing and selective targeting of the mitochondria where SuOx is located (Figure 2c). It has been shown that it is possible to selectively deliver a variety of cargos like nanoparticles,[20] liposomes[21] and polymers[22] to mitochondria by addition of TPP. The Dopa-TPP ligand was synthesized by amide-bond formation between dopamine hydrochloride and 5-carboxypentyl-triphenyl-phosphonium bromide and characterized by proton nuclear magnetic resonance (^{1}H NMR) and high resolution electron spray ionization mass spectrometry (HR-ESI-MS). IR and UV−vis spectroscopy (Supporting Information Figures S4 and S5) confirmed the successful surface functionalization. The nanoparticles remained well dispersible in water (up to 1 mg/mL, Figure 2a) and did not aggregate during the functionalization process (TEM, Supporting Information Figure S5, inset).

Sulfite Oxidase Activity. The SuOx activity of the MoO_3-TPP nanoparticles was investigated spectrophotometrically by measuring the reduction of potassium hexacyanoferrate(III) ($K_3[Fe(CN)_6]$, ferricyanide), which was chosen in order to exclude possible side reactions with the naturally occurring cytochrome c during *in vitro* experiments, at 420 nm in deionized water.[23] In the presence of different concentrations of MoO_3-TPP (0−0.04 mg/mL) with fixed concentrations of sulfite (0.66 mM) a linear dependence of the rate of ferricyanide (0.33 mM) reduction was observed (Figure 3a, blue diamonds). When the nanoparticles were replaced by bulk MoO_3 under otherwise identical experimental conditions, a significantly lower SuOx activity was observed (Figure 3b, orange diamonds), highlighting the enhanced reactivity of the nanomaterial. Unfunctionalized calcinated MoO_3 nanoparticles assayed under identical conditions (Supporting Information Figure S6) showed a higher SuOx activity than bulk MoO_3, but a significantly lower activity than functionalized MoO_3-TPP nanoparticles.

We next varied the concentration of sulfite while keeping the concentrations of MoO_3-TPP nanoparticles (0.025 mg/mL) and ferricyanide (0.3 mM) constant. A sigmoidal behavior toward sulfite was observed, which is typical for cooperative binding of substrates to the active site (Figure 3). A possible explanation could be that sulfite anions are competing with negatively charged ferricyanide on the nanoparticle surface. Additional experiments, where the concentration of ferricyanide was varied (0.015−0.6 mM) and the concentrations of MoO_3-TPP (0.025 mg/mL) and sulfite (0.66 mM) were constant, showed a linear dependence with no cooperativity (Supporting Information Figure S7), suggesting that ferricyanide stabilizes the inactive Mo^{IV} oxidation state. This was also observed for the native enzyme and model complexes of

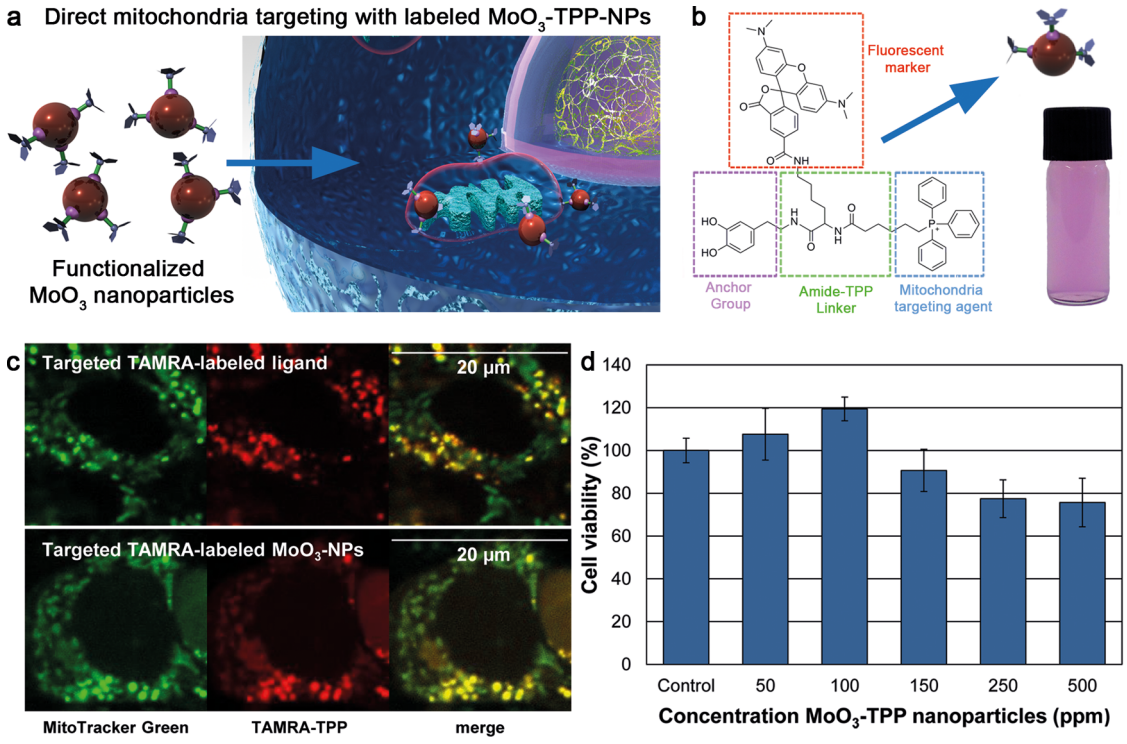

Figure 4. Mitochondria targeting of MoO_3-TPP nanoparticles and colocalization with MitoTracker Green. (a) Schematic representation of mitochondria targeting of TAMRA-labeled MoO_3-TPP nanoparticles. (b) Surface functionalization of 2 nm MoO_3 nanoparticles with ligand additionally containing TAMRA as fluorescent marker. (c) LSM colocalization studies in HepG2 cells using MitoTracker Green (50 nM, 30 min, λ_{ex} = 488 nm) with TAMRA-labeled MoO_3-TPP nanoparticles (MoO_3-TAMRA-TPP, 50 ppm, 8 h, λ_{ex} = 543 nm) and TAMRA-labeled ligand (Dopa-TAMRA-TPP, 50 ppm, 8 h, λ_{ex} = 543 nm) showing selective targeting of the mitochondria by colocalization with MitoTracker Green (merge). (d) Cytotoxicity assay with MoO_3-TPP nanoparticles after 24 h showing low toxicity up to 500 ppm.

SuOx.[24] Figure 3c shows a mechanistic proposal for the SuOx activity of MoO_3 nanoparticles in the presence of sulfite and ferricyanide. A Mo^V intermediate was detected in native SuOx by electron paramagnetic resonance spectroscopy (EPR).[23] No Mo^V EPR signal could be observed in the Moco-containing enzyme arsenite oxidase derived from *Alcaligenes faecalis*[25] or for the reaction of MoO_3-TPP (0.0025 mg/mL) nanoparticles with sulfite (0.66 mM) and ferricyanide (0.3 mM) after cooling with liquid nitrogen. To demonstrate the MoO_3-promoted sulfate formation, MoO_3-TPP nanoparticles (0.1 mg/mL) were incubated with sulfite (6.6 mM) and cytochrome c (0.1 mg/mL) for 1 h at room temperature. Sulfate was precipitated by addition of barium chloride (8.5 mM), and the formation of barium sulfate ($BaSO_4$, Supporting Information Figure S8) was confirmed by IR spectroscopy.

On the basis of the Hill equation, K_m values of 0.59 ± 0.02 mM for SO_3^{2-} and a Hill coefficient n (cooperativity constant) of 2.35 ± 0.15, indicative of a positive cooperative behavior, were determined. The MoO_3-TPP nanoparticles mediate the sulfite oxidation in the presence of ferricyanide with a V_{max} of 35.23 ± 1.13 μM/min, from which a turnover frequency (k_{cat}) of 2.78 ± 0.09 s^{-1} was determined. These kinetic values have the same order of magnitude as those for goat SuOx ($K_m(SO_3^{2-})$ = 0.70 mM)[26] and the human SuOx mutant R160Q ($K_m(SO_3^{2-})$ = 1.7 mM),[27] but they are higher than that of native human SuOx ($K_m(SO_3^{2-})$ = 0.017 mM).[27] The functional inorganic model complex $[Bu_4N][Mo^{VI}O_2(mnt)_2]$ also oxidizes sulfite, but its K_m (10 mM) is significantly higher, and nonaqueous solvents are needed.[13] The k_{cat} value of the MoO_3-TPP nanoparticles is lower than the corresponding value determined for native human SuOx (k_{cat} = 16 s^{-1}),[9] but slightly higher compared to the SuOx mutant R160Q (k_{cat} = 2.4 s^{-1})[9] and still significantly higher than that for the nanoparticle haloperoxidase mimic V_2O_5 ($k_{cat} = 7.3 \times 10^{-6}$ s^{-1}).[28]

Mitochondria Targeting Experiments. In order to demonstrate the selective mitochondria targeting of the functionalized MoO_3-TPP nanoparticles (Figure 4a) the fluorescent marker 5-carboxytetramethylrhodamine (TAMRA) was incorporated into the surface ligand (Dopa-TAMRA-TPP) as illustrated in Figure 4b. We carried out two sets of controls: MoO_3 nanoparticles functionalized with the TAMRA-containing ligand but without the targeting agent TPP (MoO_3-TAMRA) and the labeled ligand (Dopa-TAMRA-TPP) alone were incubated with HepG2 cells (50 ppm, 8h, λ_{ex} = 488 nm). Laser scanning microscopy (LSM) colocalization imaging, using the mitochondria targeting fluorescent dye MitoTracker Green (50 nM, 30 min, λ_{ex} = 488 nm), showed that the presence of TPP is required to specifically

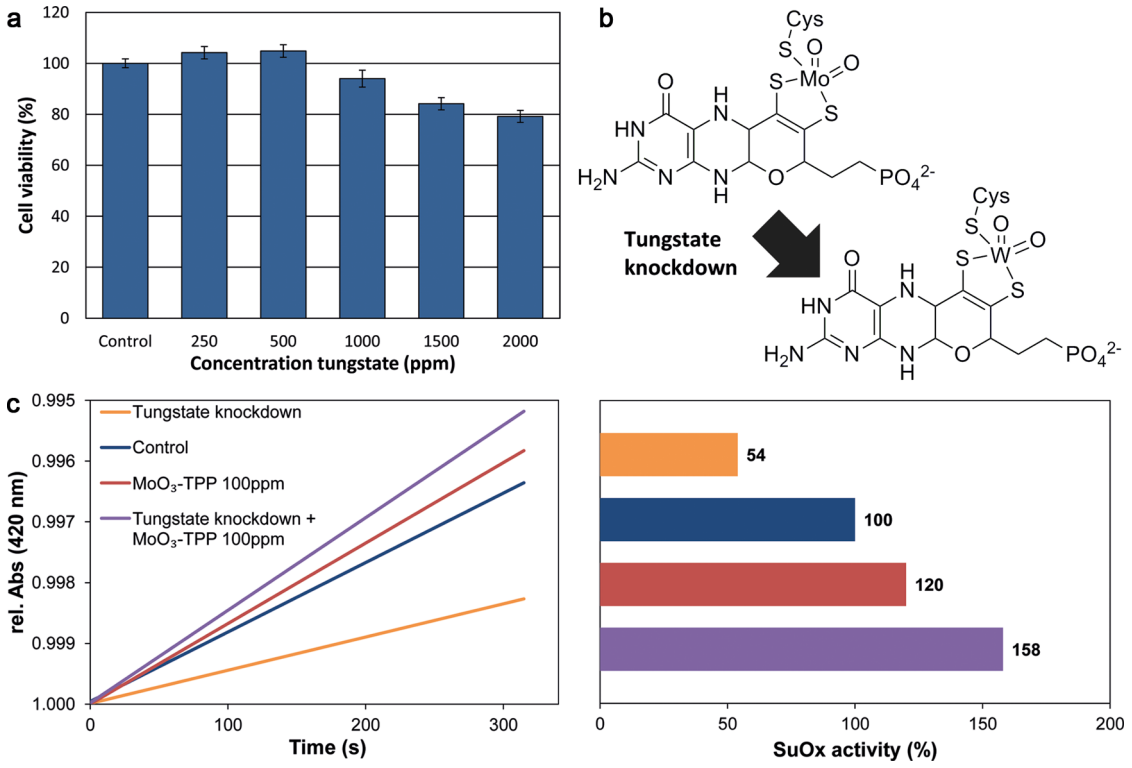

Figure 5. Chemically induced SuOx knockdown and *in vitro* SuOx activity of MoO_3-TPP nanoparticles. (a) Cytotoxicity assay with sodium tungstate after 24 h showing no toxicity up to 1000 ppm. (b) Chemically induced SuOx knockdown with sodium tungstate: Molybdenum is exchanged by tungsten in Moco leading to a significant decrease in SuOx activity.[30] (c) Best fit diagram and corresponding bar plot of *in vitro* SuOx activity of tungstate knockdown hepatocytes with functionalized MoO_3-TPP nanoparticles (100 ppm, 24 h) and sodium tungstate (250 ppm, 168 h) in the presence of constant concentrations of SO_3^{2-} (0.66 mM) and potassium ferricyanide (0.33 mM) in mitochondria lysates.

target the mitochondria. Pearson's correlation coefficient (PCC) quantitatively describes the colocalization of the two dyes. MoO_3-TAMRA nanoparticles were spread throughout the cells (Supporting Information Figure S9), whereas the Dopa-TAMRA-TPP ligand was colocalized with MitoTracker Green (Figure 4c) showing a PCC of 0.84. When incubating the fluorescently labeled MoO_3-TAMRA-TPP nanoparticles together with MitoTracker Green in HepG2 cells (50 ppm, 8h) we observed cellular uptake and selective nanoparticle targeting of the mitochondria (Figure 4c) with a PCC of 0.91. In order to consider MoO_3-TPP nanoparticles for potential biomedical applications, their cytotoxicity was assessed by coincubation with HepG2 cells for 24 h. In concentrations of 50, 100, 150, 250, and 500 ppm the percentage of cell survival was 108 ± 12, 119 ± 6, 91 ± 10, 77 ± 9, and 76 ± 11%, respectively (Figure 4d), revealing that MoO_3-TPP nanoparticles show low toxicity and could be further used within a therapeutic framework.

***In Vitro* SuOx Activity.** To test MoO_3-TPP nanoparticles with respect to their feasibility for a possible treatment of SOD, SuOx knockdown hepatocytes had to be generated. The reduction in enzyme activity is possible through genetic modification, siRNA induced gene knockdown[29] or chemical treatment with sodium tungstate, leading to a catalytically inactive analogue by replacing molybdenum with tungsten in Moco because of its higher affinity constant (Figure 5b).[30] To elucidate the possibility for a chemical knockdown using sodium tungstate, we tested the tolerance and impact of different concentrations of tungstate on the viability of HepG2 cells using a luciferase-based cytotoxicity assay. Figure 5a shows that sodium tungstate is nontoxic up to 1000 ppm. In parallel, we evaluated the degree of SuOx activity reduction, on the basis of the assumption that molybdenum will be replaced by tungstate (Figure 5b). For this purpose, we continuously treated HepG2 cells with sodium tungstate (250 ppm, 7 days, 37 °C) and observed a SuOx activity reduction down to 54% (Figure 5c, orange bar) compared to untreated control cells (Figure 5c, blue bar). In order to test if MoO_3-TPP nanoparticles could act as an enzyme replacement and recover the SuOx activity, SuOx knockdown and control cells were treated with MoO_3-TPP nanoparticles (100 ppm, 1 day, 37 °C) showing an increase of the SuOx activity in the tungstate free control (120%, Figure 5c, red bar) and a complete recovery in SuOx knockdown cells (154%, Figure 5c, purple bar).

CONCLUSION

In conclusion, we have demonstrated the ability of MoO_3 nanoparticles to oxidize sulfite to sulfate in

hepatocytes in analogy to native SuOx both *ex vivo* and *in vitro* and achieved a long-standing goal of biomimetic chemistry, the construction of an artificial enzyme, which imitates the essential and general principles of its natural counterpart.[31] Several groups have attempted to imitate the biological function of enzymes with catalysts based on coordination complexes,[32,33] and some nanomaterials were reported to exhibit enzyme-like activities.[28,34−38] The functionalized MoO_3-TPP nanoparticles were shown to cross the cellular membrane and accumulate at the mitochondria. They are highly soluble in water and have a low toxicity profile while increasing the SuOx activity in chemically induced SuOx knockdown cells. Artificial enzymes are not only useful to understand the reaction mechanism of native enzymes but also have potential applications as therapeutic agents. SOD is a rare autosomal inherited disorder of the normal degradation of sulfur-containing amino acids.[10] Premature death in infancy secondary to severe neurologic deterioration is the usual outcome. SOD originates either from gene defects encoding proteins involved in Moco biosynthesis or in the SuOx gene itself.[27] Up to now only one form of molybdenum cofactor deficiency (MoCD) can be treated by daily administration of the Moco-precursor cyclic pyranopterin monophosphate.[39,40] No other treatment for SOD or MoCD is known. As dietary treatments are not suitable for infants, this study may lay the basis for an application of MoO_3 nanoparticles for SOD therapeutic applications. In addition, it may be a corner stone for new applications in chemical biology (*e.g.*, labeling of cellular structures) or in pharmacology for the activation of molecules with low cell penetrability.

METHODS

Chemicals. 5-Carboxypentyltriphenylphosphonium bromide (5-carboxy-TPP, 97%, Alfa Aesar), *N*,*N*,*N*′,*N*′-tetramethyl-*O*-(*N*-succinimidyl)uronium tetrafluoroborate (TSTU, 97%, Aldrich), *N*,*N*-diisopropylethylamine (DIPEA, ReagentPlus, 99%, Sigma-Aldrich), *N*,*N*-dimethylformamide (DMF, ACS reagent, ≥99.8%, Sigma-Aldrich), dopamine hydrochloride (Sigma), diethyl ether (CHROMASOLV, for HPLC, ≥99.9%, inhibitor-free, Sigma-Aldrich), Fmoc-Lys(5-TAMRA)-OH (Ex/Em 544/572 nm, Biomol), piperidine (ReagentPlus, 99%, Sigma-Aldrich), molybdenum powder (purity 99.95%, Alfa Aesar), H_2O_2 (35 wt % in H_2O, Sigma-Aldrich), acetic acid (ReagentPlus, ≥99% Sigma-Aldrich), bovine serum (fetal bovine serum, Sigma), potassium hexacyanoferrate(III) ($K_3[Fe(CN)_6]$, ferricyanide, ReagentPlus, ∼99%, Sigma-Aldrich), sodium sulfite (≥98%, Sigma-Aldrich), bulk MoO_3 (ReagentPlus, ≥99.5%, Sigma-Aldrich), barium chloride (Suprapur, 99.995%, Merck), barium sulfate ($BaSO_4$, Fluka), cytochrome c (cytochrome c from equine heart, ≥95%, Sigma), 37% hydrochloric acid (ACS reagent, 37%, Sigma-Aldrich), DMEM media (Dulbecco's Modified Eagle Medium, Life Technologies Corporation), MitoTracker Green FM (Ex/Em 490/516 nm, Life Technologies Corporation) and sodium tungstate (dihydrate, purum, ≥99%, Sigma-Aldrich) were used without further purification.

Dopamine-TPP (1). 2.2 mmol of 5-carboxy-TPP, 3.5 mmol of TSTU and 6.6 mmol DIPEA were dissolved in 25 mL of DMF and stirred for 15 min at room temperature (RT). 2.6 mmol of dopamine hydrochloride were dissolved in 25 mL of DMF and added to the solution, and the mixture stirred overnight at RT. Afterward the solvents were removed, and the product precipitated in diethyl ether. The precipitate was analyzed by ^{1}H NMR, HR-ESI-MS, UV−vis, and IR. Yield: 255 mg (23%). Spectroscopic characterization: ^{1}H NMR (400 MHz, DMSO-d_6) δ 8.72 (s, 2H), 7.91−7.78 (m, 16H), 6.61 (d, J = 8 Hz, 1H), 6.55 (d, J = 2 Hz, 1H), 6.41 (dd, J = 2 Hz, 8 Hz, 1H), 3.58−3.53 (m, 2H), 3.14 (q, J = 6.9 Hz, 1H), 2.48−2.46 (m, 2H), 2.00 (t, J = 6.9 Hz, 2H), 1.51−1.41 (m, 6H); IR (neat) 3381, 2926, 1636, 1516, 1434, 1278, 1053, 722, 690, 530, 505 cm^{-1}; UV−vis λ_{max} 275 nm; HR-ESI-MS (*m*/*z*) [M]$^+$ calcd. for $C_{32}H_{35}NO_3P^+$ 512.2355, found 512.2366.

Dopamine-Lys(5-TAMRA)-Fmoc (2). 0.04 mmol of Fmoc-Lys(5-TAMRA)-OH, 0.04 mmol TSTU and 0.16 mmol DIPEA were dissolved in 5 mL of DMF and stirred for 15 min at RT. 0.05 mmol of dopamine hydrochloride were dissolved in 5 mL of DMF and added to the solution, and the mixture stirred overnight at RT. Afterward the solvents were removed, and the product precipitated in diethyl ether. The precipitate was analyzed by ^{1}H NMR, HR-ESI-MS, and UV−vis. Yield: 20 mg (56%). Spectroscopic characterization: ^{1}H NMR (400 MHz, MeOD-d_4) δ 8.71 (s, 1H), 8.18 (d, J = 8 Hz, 1H), 7.76−7.62 (m, 4H), 7.31−7.26 (m, 5H), 7.05−6.91 (m, 6H), 6.76−6.49 (m, 6H), 4.32 (d, J = 6.9 Hz, 2H), 4.16 (d, J = 7.1 Hz, 1H), 4.04 (m, 1H), 3.49 (t, J = 6.3 Hz, 2H), 3.27 (s, 12H), 3.09 (t, J = 7.6 Hz, 1H), 2.79 (t, J = 7.6 Hz, 1H), 2.62 (t, J = 7.1 Hz, 2H), 1.77−1.68 (m, 4H), 1.48−1.42 (m, 2H); UV−vis λ_{max} 547 nm; HR-ESI-MS (*m*/*z*) [M + H]$^+$ calcd. for $C_{54}H_{54}N_5O_9^+$ 916.3922, found 916.3890.

Dopamine-Lys(5-TAMRA)-TPP (3). 0.01 mmol of **2** were dissolved in 10 mL of 20% piperidine in DMF, stirred for 1 h, and precipitated in diethyl ether. 0.005 mmol 5-carboxy-TPP, 0.005 mmol TSTU, and 0.02 mmol DIPEA were dissolved in 5 mL of DMF and stirred for 15 min at RT. The precipitate was dissolved in 5 mL of DMF and added to the solution, and the mixture stirred overnight at RT. Afterward the solvents were removed, and the product precipitated in diethyl ether. The precipitate was analyzed by ^{1}H NMR, HR-ESI-MS, and UV−vis. Yield: 5 mg (23%). Spectroscopic characterization: ^{1}H NMR (400 MHz, DMSO-d_6) δ 8.80−8.65 (m, 3H), 8.42 (s, 1H), 8.32 (m, 2H), 8.21 (s, 1H), 7.89−7.78 (m, 15H), 7.30 (s, 1H), 6.62−6.40 (m, 9H), 4.10−4.04 (m, 3H), 3.64−3.52 (m, 4H), 3.17 (m, 4H), 2.95 (s, 12H), 1.96 (t, J = 6.9 Hz, 2H), 1.96−1.52 (m, 12H); UV−vis λ_{max} 549 nm; HR-ESI-MS (*m*/*z*) [M]$^+$ calcd. for $C_{63}H_{67}N_5O_8P^+$ 1052.4727, found, 1052,4716.

MoO_3 Nanoparticles. MoO_3 nanoparticles were synthesized as described elsewhere.[18] In brief, 10.4 mmol of molybdenum powder and 10 mL of H_2O_2 were dissolved in 12 mL of distilled water and cooled to 0 °C. Two milliliters of acetic acid were added dropwise under rigorous stirring. The solvents were removed *in vacuo*, and the yellow precipitate was washed with distilled water and ethanol. Finally, the yellow product was dried *in vacuo* and afterward heated to 450 °C for 30 min. A bluish powder was obtained, which was analyzed by TEM, STEM, EDX, P-XRD, UV−vis, and IR. To test the stability in serum MoO_3 nanoparticles were dispersed in bovine serum and incubated for 6 h at RT. Afterward the nanoparticles were separated by ultracentrifugation, washed with distilled water and ethanol, dried *in vacuo*, and analyzed by P-XRD (Supporting Information Figure S3).

Surface Functionalization of MoO_3 Nanoparticles. The synthesized MoO_3 nanoparticles were dispersed in DMF under argon. A solution of the ligand (1, 2, or 3) in DMF was added, and the mixture stirred for 3 h at RT. The solvent was removed *in vacuo*, and the precipitate was washed with distilled water and ethanol and dried *in vacuo*. The result of the surface functionalization was controlled by UV−vis and IR spectroscopy.

Sulfite Oxidase Activity. The SuOx activity of the MoO_3 nanoparticles was determined spectrophotometrically using ferricyanide as electron acceptor, by measuring the initial reduction

rates at 420 nm ($\varepsilon_{420\ nm}$ = 1.04 mM^{-1} cm^{-1})[22] on a Cary 5G UV−vis−NIR spectrophotometer (Varian Inc., Palo Alto, CA, USA) after sulfite addition. Typically, the SuOx activity was measured in Milli-Q water by varying the concentration of MoO_3 nanoparticles (0−0.04 mg/mL) and keeping the concentrations of ferricyanide (0.3 mM) and sodium sulfite (0.66 mM) constant for 180 s at 25 ± 2 °C. The slight background reaction between MoO_3 and ferricyanide was subtracted from the reaction rate obtained after sulfite addition. As controls, the following experiments were performed: (i) bulk MoO_3 (0−0.04 mg/mL) and (ii) by keeping the concentration of MoO_3 nanoparticles (0.025 mg/mL), sodium sulfite (0.66 mM) constant and varying the concentrations of ferricyanide (0.015−0.6 mM). Mean values of the initial ferricyanide reduction rates of three traces were used in the calculations.

Determination of Kinetic Parameters. The steady-state kinetic experiments were carried out by measuring the initial rates of the ferricyanide reduction at 420 nm in Milli-Q water for 180 s at 25 ± 2 °C on a Cary 5G UV−vis−NIR spectrophotometer. For this purpose the concentration of sodium sulfite was varied from 0.033 to 1.65 mM while keeping the concentrations of ferricyanide (0.3 mM) and MoO_3-TPP nanoparticles (0.025 mg/mL) constant. Mean values of the initial ferricyanide reduction rates of three traces were used in the calculations. The initial rate values were adjusted to the Michaelis−Menten model and the Hill equation. Kinetic parameters were calculated using the software Sigma-Plot with the module enzyme kinetics (Systat Software Inc.). The k_{cat} was determined as follows: $k_{cat} = V_{max}/[MoO_3]$, where MoO_3 nanoparticle concentration was determined by using the average nanoparticle diameter (TEM) as described elsewhere.[41] The average diameter was converted to the spherical volume and the mass $m(MoO_3\ NP)$ of a single particle (1.97×10^{-20} g) attained by multiplication with the density of bulk MoO_3 (4.7 g/cm^{-3}). Afterward $[MoO_3]$ was determined as follows: $[MoO_3] = C_m/m(MoO_3\ NP) \times N_A$, where C_m is the mass concentration used during the assay and N_A the Avogadro constant.

Physical Characterization. Low-resolution TEM images of the nanoparticles were obtained on a Philips 420 instrument with an acceleration voltage of 120 kV. STEM and EDX data were obtained on a FEI Tecnai F30 S-TWIN with a 300 kV field emission gun equipped with an Oxford EDX spectrometer with a Si/Li detector and an ultrathin window for elemental analysis. P-XRD was carried out on a Siemens D5000 diffractometer equipped with a Braun M50 position sensitive detector in transmission mode using Cu Kα radiation and analyzed using EVA software. UV−vis spectra were recorded on a Cary 5G UV−vis−NIR spectrophotometer in a range from 200 to 600 nm. IR experiments were conducted on a Bruker Alpha-P FT-IR spectrometer with Platinum-ATR (Bruker, Billerica, MA, USA).

Determination of $BaSO_4$. Sulfate production was confirmed by IR after precipitation with barium chloride on a Bruker Alpha-P FT-IR and compared to commercial $BaSO_4$. For this purpose sodium sulfite (6.6 mM), cytochrome c (0.1 mg/mL), and MoO_3-TPP nanoparticles (0.1 mg/mL) were incubated for 60 min in distilled water. Afterward 2 μL of 37% hydrochloric acid per milliliter of reaction mix was added, and the sulfate precipitated by addition of barium chloride (8.5 mM). The precipitate was isolated by ultracentrifugation, air-dried, and analyzed by IR.

LSM Uptake and Localization Studies. HepG2 cells were cultured in DMEM media supplemented with 10% FCS and 1% L-glutamine. Cells were maintained at 37 °C and 5% CO_2 until reaching 70% of confluence. For uptake and colocalization studies, 1×10^4 cells were plated in Lab-Tek 8-well chamber slides (Thermo Fisher Scientific, Waltham, MA, USA) and grown for 24 h. Afterward the cells were treated with 50 ppm of fluorescent MoO_3-TAMRA/MoO_3-TAMRA-TPP nanoparticles or Dopa-TAMRA-TPP ligand, respectively, for 8 h. For colocalization studies the cells were stained with MitoTracker Green FM with a final concentration of 50 nM 30 min prior to laser scanning experiments. For cellular imaging a confocal laser scanning microscope (Zeiss LSM-710-NLO equipped with Zeiss LSM Zen software, Carl Zeiss, Jena, Germany) with λ_{ex} = 488 nm and λ_{ex} = 543 nm was used. PCCs were calculated using the program ImageJ (with PSC colocalization plug-in) using a previously described protocol.[42]

Cytotoxicity Assay. 1×10^4 HepG2 cells were cultured in a 96 well plate and grown for 24 h at 37 °C and 5% CO_2. Afterward TPP-functionalized MoO_3 nanoparticles (50, 100, 150, 250, 500, 750, and 1000 ppm) or sodium tungstate (250, 500, 1000, 1500, and 2000 ppm) were added, and cell viability was determined by CellTiter-Glo viability assay kit (Promega, Madison, WI, USA) according to manufacturer instructions and measured by Tecan i-control infinite 200 (Tecan, Männedorf, Switzerland). The experiments were performed in duplicate.

***In Vitro* SuOx Activity.** 1×10^8 HepG2 cells were cultured in 250 mL flasks (Greiner Bio-One, Frickenhausen, Germany) and grown for 7 days at 37 °C and 5% CO_2. SuOx knockdown cells were generated by addition of sodium tungstate (250 ppm, 7 days), whereas functionalized MoO_3-TPP nanoparticles were added (100 ppm,1 day) in recovery experiments. Cells were harvested after 7 days, and the mitochondria isolated by ultracentrifugation using a Mitochondria Isolation Kit (Sigma) according to manufacturer instructions. The mitochondria were resuspended in lysis buffer (250 mM Tris-HCl, 1 mM EDTA and 0.2% sodium desoxycholate) for 15 min on ice. The total protein concentration of the individual fractions was determined using Roti-Nanoquant (Carl-Roth, Karlsruhe, Germany) with bovine serum albumin as standard according to manufacturer instructions, by determination of OD_{590}/OD_{450} with Tecan i-control infinite 200. The SuOx activity of the individual fractions was determined spectrophotometrically, by measuring the reduction rates of ferricyanide at 420 nm on a Tecan i-control infinite 200. Typically, the SuOx activity was measured in buffer containing 250 mM Tris-HCl, 1 mM EDTA and 0.1% sodium desoxycholate by keeping the concentrations of ferricyanide (0.3 mM) and sodium sulfite (0.66 mM) constant for 315 s at 25 ± 2 °C. The slight background reaction between the lysates and ferricyanide was subtracted from the reaction rate obtained after sulfite addition. The SuOx activities were normalized according to the total protein concentrations of the individual fractions.

Conflict of Interest: The authors declare no competing financial interest.

Acknowledgment. This research was partially supported by the Naturwissenschaftlich-medizinisches Forschungszentrum (NMFZ) Mainz, the DFG within the SPP 1313, and the Max Planck Graduate School (MPGC).

Supporting Information Available: P-XRD and aqueous dispersions of as-synthesized and calcinated MoO_3 NPs, P-XRD of MoO_3 NPs after bovine serum incubation, IR/UV−vis spectra and TEM-image after functionalization, SuOx activity of unfunctionalized MoO_3 NPs, SuOx activity dependence on ferricyanide concentration, IR spectra of $BaSO_4$ formed after SuOx reaction, LSM localization of untargeted MoO_3 NPs, ^1H NMR spectra of synthesized Dopa-ligands. This material is available free of charge *via* the Internet at http://pubs.acs.org.

REFERENCES AND NOTES

1. Haber, J.; Lalik, E. Catalytic Properties of MoO_3 Revisited. *Catal. Today* **1997**, *33*, 119–137.
2. Grasselli, R. K. Fundamental Principles of Selective Heterogeneous Oxidation Catalysis. *Top. Catal.* **2002**, *21*, 79–88.
3. Di Gregorio, F.; Keller, V. Activation and Isomerization of Hydrocarbons over WO_3/ZrO_2 Catalysts: I. Preparation, Characterization, and X-ray Photoelectron Spectroscopy Studies. *J. Catal.* **2004**, *225*, 45–55.
4. Gutierrez, O. Y.; Perez, F.; Fuentes, G. A.; Bokhimi, X.; Klimova, T. Deep HDS over NiMo/Zr-SBA-15 Catalysts with Varying MoO_3 Loading. *Catal. Today* **2008**, *130*, 292–301.
5. Aoki, K.; Ohmae, M.; Nanba, T.; Takeishi, K.; Azuma, N.; Ueno, A.; Ohfune, H.; Hayashi, H.; Udagawa, Y. Direct Conversion of Methane into Methanol over MoO_3/SiO_2 Catalyst in an Excess Amount of Water Vapor. *Catal. Today* **1998**, *45*, 29–33.
6. Pilato, R. S.; Stiefel, E. I. In *Bioinorganic Catalysis*, 2nd ed.; Reedijk, J., Bouwman, E., Eds.; Marcel Dekker: New York, 1999; pp 81−152.

7. Hille, R. The Molybdenum Oxotransferases and Related Enzymes. *Dalton Trans.* **2013**, *42*, 3029–3042.
8. Schwarz, G.; Mendel, R. R.; Ribbe, M. W. Molybdenum Cofactors, Enzymes and Pathways. *Nature* **2009**, *460*, 839–847.
9. Garrett, R. M.; Johnson, J. L.; Graf, T. N.; Feigenbaum, A.; Rajagopalan, K. V. Human Sulfite Oxidase R160Q: Identification of the Mutation in a Sulfite Oxidase-Deficient Patient and Expression and Characterization of the Mutant Enzyme. *Proc. Natl. Acad. Sci. U. S. A.* **1998**, *95*, 6394–6398.
10. Arnold, G. L.; Greene, C. L.; Patrick Stout, J.; Goodman, S. I. Molybdenum Cofactor Deficiency. *J. Pediatr.* **1993**, *123*, 595–598.
11. Xiao, Z.; Young, C. G.; Enemark, J. H.; Wedd, A. G. A Single Model Displaying all the Important Centers and Processes Involved in Catalysis by Molybdoenzymes Containing $[Mo^{VI}O_2]^{2+}$ Active Sites. *J. Am. Chem. Soc.* **1992**, *114*, 9194–9195.
12. Groysman, S.; Holm, R. H. Biomimetic Chemistry of Iron, Nickel, Molybdenum, and Tungsten in Sulfur-Ligated Protein Sites. *Biochemistry* **2009**, *48*, 2310–2320.
13. Das, S. K.; Chaudhury, P. K.; Biswas, D.; Sarkar, S. Modeling for the Active Site of Sulfite Oxidase: Synthesis, Characterization, and Reactivity of $[MoVIO_2(mnt)_2]^{2-}$ (mnt^{2-} = 1,2-Dicyanoethylenedithiolate). *J. Am. Chem. Soc.* **1994**, *116*, 9061–9070.
14. André, R.; Natálio, F.; Tremel, W. Nanoparticles as Enzyme Mimics. In *New and Future Developments in Catalysis*; Suib, S. L., Ed.; Elsevier: Amsterdam, 2013; Chapter 6, pp 149−173.
15. Wei, H.; Wang, E. Nanomaterials with Enzyme-Like Characteristics (Nanozymes): Next-Generation Artificial Enzymes. *Chem. Soc. Rev.* **2013**, *42*, 6060–6093.
16. Ressler, T.; Wienold, J.; Jentoft, R. E.; Girgsdies, F. Evolution of Defects in the Bulk Structure of MoO_3 during the Catalytic Oxidation of Propene. *Eur. J. Inorg. Chem.* **2003**, *2*, 301–312.
17. Zollfrank, C.; Gutbrod, K.; Wechsler, P.; Guggenbichler, J. P. Antimicrobial Activity of Transition Metal Acid MoO_3 Prevents Microbial Growth on Material Surfaces. *Mater. Sci. Eng., C* **2012**, *32*, 47–54.
18. Redel, E.; Petrov, S.; Dag, Ö.; Moir, J.; Huai, C.; Mirtchev, P.; Ozin, G. A. Green Nanochemistry: Metal Oxide Nanoparticles and Porous Thin Films from Bare Metal Powders. *Small* **2012**, *8*, 68–72.
19. Morvaj, J.; Ban, Z. Composition and Structure of Molybdenum Peroxide. *Z. Kristallogr.* **1988**, *185*, 489.
20. Marrache, S.; Dhar, S. Engineering of Blended Nanoparticle Platform for Delivery of Mitochondria-Acting Therapeutics. *Proc. Natl. Acad. Sci. U. S. A.* **2012**, *109*, 16288–16293.
21. Zhou, J.; Zhao, W.-Y.; Ma, X.; Ju, R.-J.; Li, X.-Y.; Li, N.; Sun, M.-G.; Shi, J.-F.; Zhang, C.-X.; Lu, W.-L. The Anticancer Efficacy of Paclitaxel Liposomes Modified with Mitochondrial Targeting Conjugate in Resistant Lung Cancer. *Biomaterials* **2013**, *34*, 3626–3638.
22. Callahan, J.; Kopeček, J. Semitelechelic HPMA Copolymers Functionalized with Triphenylphosphonium as Drug Carriers for Membrane Transduction and Mitochondrial Localization. *Biomacromolecules* **2006**, *7*, 2347–2356.
23. Cohen, H. J.; Fridovich, I. Hepatic Sulfite Oxidase: Purification and Properties. *J. Biol. Chem.* **1971**, *246*, 359–366.
24. Helton, M. E.; Kirk, M. L. A Model for Ferricyanide-Inhibited Sulfite Oxidase. *Inorg. Chem.* **1999**, *38*, 4384–4385.
25. Hoke, K. R.; Cobb, N.; Armstrong, F. A.; Hille, R. Electrochemical Studies of Arsenite Oxidase: An Unusual Example of a Highly Cooperative Two-Electron Molybdenum Center. *Biochemistry* **2004**, *43*, 1667–1674.
26. Ahmad, A.; Ahmad, S.; Baig, M. A. Purification and Characterization of Sulfite Oxidase from Goat Liver. *Indian J. Biochem. Biophys.* **2008**, *6*, 379–386.
27. Karakas, E.; Wilson, H. L.; Graf, T. N.; Xiang, S.; Jaramillo-Busquets, S.; Rajagopalan, K. V.; Kisker, C. Structural Insights into Sulfite Oxidase Deficiency. *J. Biol. Chem.* **2005**, *280*, 33506–33515.
28. Natalio, F.; Andre, R.; Hartog, A. F.; Stoll, B.; Jochum, K. P.; Wever, R.; Tremel, W. Vanadium Pentoxide Nanoparticles Mimic Vanadium Haloperoxidases and Thwart Biofilm Formation. *Nat. Nanotechnol.* **2012**, *7*, 530–535.
29. Brychkova, G.; Xia, Z.; Yang, G.; Yesbergenova, Z.; Zhang, Z.; Davydov, O.; Fluhr, R.; Sagi, M. Sulfite Oxidase Protects Plants against Sulfur Dioxide Toxicity. *Plant J.* **2007**, *50*, 696–709.
30. Johnson, J. L.; Rajagopalan, K. V.; Cohen, H. J. Molecular Basis of the Biological Function of Molybdenum: Effect of Tungsten on Xanthine Oxidase and Sulfite Oxidase in the Rat. *J. Biol. Chem.* **1974**, *249*, 859–866.
31. Breslow, R.; Overman, L. E. "Artificial Enzyme" Combining a Metal Catalytic Group and a Hydrophobic Binding Cavity. *J. Am. Chem. Soc.* **1970**, *92*, 1075–1077.
32. Lippard, S. J. The Inorganic Side of Chemical Biology. *Nat. Chem. Biol.* **2006**, *2*, 504–507.
33. Zastrow, M. L.; Peacock, A. F. A.; Stuckey, J. A.; Pecoraro, V. L. Hydrolytic Catalysis and Structural Stabilization in a Designed Metalloprotein. *Nat. Chem.* **2012**, *4*, 118–123.
34. Chen, J.; Patil, S.; Seal, S.; McGinnis, J. F. Rare Earth Nanoparticles Prevent Retinal Degeneration Induced by Intracellular Peroxides. *Nat. Nanotechnol.* **2006**, *1*, 142–150.
35. Gao, L.; Zhuang, J.; Nie, L.; Zhang, J.; Zhang, Y.; Gu, N.; Wang, T.; Feng, J.; Yang, D.; Perrett, S.; *et al.* Intrinsic Peroxidase-Like Activity of Ferromagnetic Nanoparticles. *Nat. Nanotechnol.* **2007**, *2*, 577–583.
36. André, R.; Natálio, F.; Humanes, M.; Leppin, J.; Heinze, K.; Wever, R.; Schröder, H. C.; Müller, W. E. G.; Tremel, W. V_2O_5 Nanowires with an Intrinsic Peroxidase-Like Activity. *Adv. Funct. Mater.* **2011**, *21*, 501–509.
37. Yusop, R. M.; Unciti-Broceta, A.; Johansson, E. M. V.; Sánchez-Martín, R. M.; Bradley, M. Palladium-Mediated Intracellular Chemistry. *Nat. Chem.* **2011**, *3*, 239–243.
38. Kim, C. K.; Kim, T.; Choi, I.-Y.; Soh, M.; Kim, D.; Kim, Y.-J.; Jang, H.; Yang, H.-S.; Kim, J. Y.; Park, H.-K.; *et al.* Ceria Nanoparticles That Can Protect against Ischemic Stroke. *Angew. Chem.* **2012**, *124*, 11201–11205; *Angew. Chem., Int. Ed.* **2012**, *51*, 11039–11043.
39. Schwarz, G.; Santamaria-Araujo, J. A.; Wolf, S.; Lee, H.-J.; Adham, I. M.; Gröne, H.-J.; Schwegler, H.; Sass, J. O.; Otte, T.; Hänzelmann, P.; *et al.* Rescue of Lethal Molybdenum Cofactor Deficiency by a Biosynthetic Precursor from *Escherichia coli*. *Hum. Mol. Genet.* **2004**, *13*, 1249–1255.
40. Veldman, A.; Santamaria-Araujo, J. A.; Sollazzo, S.; Pitt, J.; Gianello, R.; Yaplito-Lee, J.; Wong, F.; Ramsden, C. A.; Reiss, J.; Cook, I.; *et al.* Successful Treatment of Molybdenum Cofactor Deficiency Type A with cPMP. *Pediatrics* **2010**, *125*, 1249–1254.
41. Korsvik, C.; Patil, S.; Seal, S.; Self, W. T. Superoxide Dismutase Mimetic Properties Exhibited by Vacancy Engineered Ceria Nanoparticles. *Chem. Commun.* **2007**, *10*, 1056–1058.
42. French, A. P.; Mills, S.; Swarup, R.; Bennett, M. J.; Pridmore, T. P. Colocalization of Fluorescent Markers in Confocal Microscope Images of Plant Cells. *Nat. Protoc.* **2008**, *3*, 619–628.